THE RELATION BETWEEN THE MICROSTRUCTURE OF CARBON STEEL (0.24 C% & 0.38 C%) AND CORROSION PROTECTION

S.R. SELIM[*(1)], A. A. MOHAMED[(1)], G.A. Al-Hazmi[(2)] and A. H. Ali[(2)]

(1) Chemistry Department, Faculty of Science, Al-Azhar University, Cairo, EGYPT.
(2) Chemistry Department, Faculty of Science, Taiz University, Taiz, YEMEN

* The present address is Chemistry Department, Faculty of science, Taiz University, Taiz, YEMEN.
* To whom corresponds should be addressed.

Abstract

The effect of carbon percent on the corrosion of steel in ethanol – aqueous H_2SO_4 solution has been studied by using weight loss technique. The effect of presence of foreign atoms in steel composition on the corrosion resistance has been investigated. Beside that, the effect of heat treatment on the corrosion rates has been interpreted. The inhibitive action of N, N-dihydroxy ethyl acryl-amide on the corrosion rate of steel appears high efficiency for all samples in all cases under study. The corrosion behavior is interpreted in view of the microstructure of samples before and after heat treatment. There are two wet corrosion processes that affected by carbon percent in the localized area. Before heat treatment the corrosion rate is more dependent upon inter-granular corrosion type while, increasing C % or by quenching regime the corrosion rate is more dependent upon allotropic–galvanic corrosion type. The corrosion rate in absence of inhibitors classified as cathodic control while it classified as cathodic–anodic control in presence of inhibitor.

Key words: steel microstructure, corrosion of low and medium carbon steel, N, N-dihydroxy ethyl acryl-amide, heat treatment.
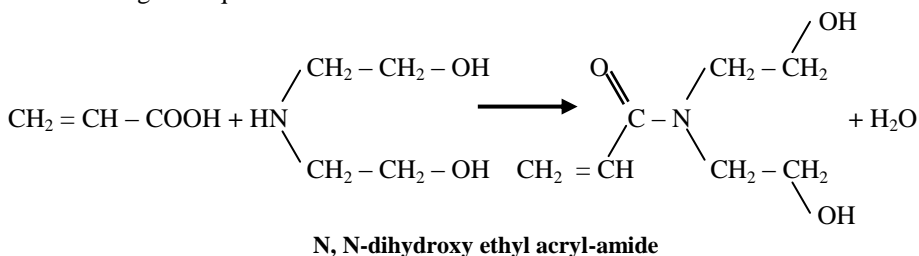
Introduction

The importance of studding the corrosion behavior of low and medium carbon steel is attributed to its widespread uses in manufactory pipes, tubes and public uses; it is used in different media and different operating. The electrochemical behavior of huge, low and medium carbon steel compounds of different composition in different media was studied [1-3]. A different heat treatment regimes are applied on steel to increase its corrosion resistance, hardens, tensile strength, and so on [4]. Many studies and applications occurred to use inhibitor additives during the operating processes to retard or prevent the corrosion of steel[5-11]. There are numerous studies for clarify the effect of acid solutions on the corrosion [5,14], in absence or in presence of different organic solvent. The corrosion rate of steel at different temperatures were determined which the effect of temperature on the adsorption of the inhibitor, was investigated[11,16]. The corrosion protection and inhibitor

efficiency of N, N-dihydroxy ethyl acryl-amide (HEAA) on gray cast steel in H_2SO_4 show fairly good results. The thermodynamic parameters, of activation and adsorption processes at different temperatures were estimated [11, 16].

   The present study is concerned with the corrosion of low and medium carbon steel in alcoholic- aqueous sulphouric acid solution. The effect of carbon percent was studied to clarify the relation between corrosion rate and steel microstructure. The effects of heat treatment of steel samples, on the corrosion resistance and on the efficiency of inhibitor are interpreted.

Experimental
Materials

1. Sulphouric acid (H_2SO_4) from A.R. reagent.

2. Potassium hydrogen phthalate (KH-phthalate) from Merck.

3. Ethanol (BDH) laboratory supplies. Poole, BH15 1TD, England.

4. Potassium permanganate ($KMnO_4$) from LOBA chemie.

5. N,N-dihydroxy ethyl acryl-amide (HEAA) was prepared previously [11] according this equation :

$$CH_2 = CH - COOH + HN\begin{array}{c} CH_2 - CH_2 - OH \\ \\ CH_2 - CH_2 - OH \end{array} \quad \xrightarrow{\hspace{2cm}} \quad \underset{CH_2\ =\ CH}{\overset{O}{\underset{\|}{C}} - N}\begin{array}{c} CH_2 - CH_2 \\ \\ CH_2 - CH_2 \end{array}\begin{array}{c} OH \\ \\ \\ OH \end{array} + H_2O$$

N, N-dihydroxy ethyl acryl-amide

   Two types of carbon steel samples have 2 cm^2 cross-section area were used, see (Table 1), where both types are; one is as cast and other heat treated by quenching regime.

Preparation of solutions

   1- Different concentrations of inhibitor (HEAA) are used (2, 4, 6, 8 and 10 x 10^{-5} Molar).

   2- The corrosive media were prepared from analytical grade chemical reagents and used without further purification. Different concentration of H_2SO_4 and ethanol were mixed (Table 2).

Methods of collecting data

The weight loss technique was applied for all samples where, the metal sample is immersed in 50 ml of corrosive medium, at the required temperature. After 2 hours, the sample is taken off from solution and washed by distilled water carefully. Remain solution is contained corroded iron as ferrous ion Which it's concentration was determined by titrated against (0.1N) $KMnO_4$ standard solution.

Result

Calculation of weight-loss of iron

The weight loss of iron is determined by redox titration method as following;

$$2KMnO_4 + 10FeSO_4 + 8H_2SO_4 \rightarrow 5Fe_2(SO_4)_3 + 2MnSO_4 + K_2SO_4 + 8H_2O \quad (1)$$
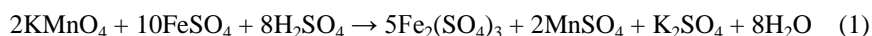
And the strength of Fe $= (N \times V_L)_{KMnO4} \times (Eq.Wt)_{Fe} = weight\text{-}loss (W)$.

$W = (0.1 \times V_{ml} \times 10^{-3}) \times 56.6 \ g$

Calculation of rate of corrosion

The rate of corrosion in (mm/y) was calculated[17], by using the following equation:

Rate of corrosion(R) = (k x W) / (A x t x D)

Where (k) is constant $= (8.76 \times 10^4)$, (A) cross-section area, (t) time (2 hours) and (D) density of iron (7.86 g/cm^3). The area is investigated according to iron percent in the samples where Fe% in LCA = 98.6% and Fe% in MCA = 98.1%.

So, $A_{LCA} = 2 \times 0.986 = 1.972 \ cm^2$, and;

$A_{MCA} = 2 \times 0.981 = 1.962 \ cm^2$,

The corrosion rates data in absence and in presence of inhibitor at 25°C was recorded in (Table 3&4).

Discussion:

Microstructure of low and medium carbon steel

Two types of steel were selected for the present study, low and medium carbon steel, which appears as iron carbide in ferritic-pearlitic phase lamina.

Manganese and sulphur did not have any significant effect on the resistance to inter-granular attack [18]. However, phosphorous and silicon were found to have a significant effect [18]. For example, the presence of phosphorous and silicon in

stainless steel has definite ratio (P < 1000 and Si < 1000 or Si ≈ 100000 ppm) reduces the inter-granular corrosion (IGC) sensitization.

The P% and Si% of LCA set the sample in moderate IGC sensitization region while, P% of MCA sets the sample in no IGC sensitization region.

According to (temperature – time sensitization) TTS curves, the high fast cooling rate between (850 – 500°C.) is highly necessary to prevent IGC sensitization [18]. The quenching heat treatment (in water) causes phase – transformation that affects the corrosion and corrosion protect action.

Microstructure of LCA & MCA before heat treatment

Microstructure of steel samples (LCA and MCA) were examined using optical microscope (micrographs) by using optical microscope technique (Nikon, made in Japan), which given in (Fig 2i , 2ii).

The microstructure of carbon steel before heat treatment is illustrated from phase diagram (Fig 1) as ferritic-pearlitic matrix. Some ferrite phase was precipitated in grains boundary and pearlite phase consists of two combined components [3, 5] (ferrite and cementite) that presence as two types of laminas (ferrite and cementite laminas).

Microstructure of LCH & MCH after heat treatment

The microstructure of carbon steel after heat treatment is illustrated from phase diagram (Fig 1, a & b heat treatment areas), where during heat treatment process (hardening regime by quenching in water) the microstructure of carbon steel were transformed from ferritic-pearlitic to martensite phase, which shown in (Fig; 3iii , 3iv). The martensite phase has small ferrite particles which distributed in between partitioned cementite laminas.

The martensite phase may be contains trace of (austenite ferrite) phase that collected during cooling period in the bulk. The ratio of (ferrite/cementite) area is changed to higher one where, the type of corrosion is more dependent upon galvanic corrosion.

**Effect of carbon percentage on corrosion behavior**

In general, the corrosion rates which calculated for the samples in absence and presence of (HEAA) under the studied conditions were increased according to the following order:

MCA> MCH> LCA> LCH. These results indicate that the corrosion rate increased with increasing carbon percent while, the heat treatment decreases the corrosion rates.

In the light of this order, we can assure that the heat treatment regime (quenching) is resisting itself the corrosion processes.

According to iron-carbon phase diagram [19] and microstructure of iron-carbon, the formed iron carbide, is present as ferritic phase and ferritic lamina in pearlitic phase. There are tow wet corrosion processes that affected by carbon percent in the localized area.

Firstly, the iron carbide of ferritic phase in grain boundary acts as anodic site against pearlitic grain matrix refers to inter-granular corrosion (IGC) type. It can be represented as;

<div align="center">Fe, grain-boundary | wet medium | pearlitic grain, Fe</div>
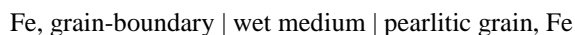
Secondary, the iron carbide of ferritic lamina in pearlitic grains acts as anodic site against cementite lamina, that giving allotropic–galvanic corrosion (AGC) type. It can be represented as;

<div align="center">Fe, Ferritic lamina | wet medium | cementite lamina, Fe</div>

In spite of phosphorous ratio percent in MCA ($0.019\% \approx 1.9 \times 10^2$ ppm) reduce the (IGC) sensitization[19], the resultant corrosion rate of medium carbon steel is higher than the corrosion rate of low carbon steel which is refer to high effect of allotropic–galvanic corrosion (AGC) owing to higher percent of ferrite/cementite ratio.

(Figure 4a), shows that the corrosion rates increased as C% increased. It is obvious the corrosion rate in absence of inhibitors depends on the Fe_3C present and classified as cathodic control.

Effect of heat treatment on corrosion behavior

(Figure 4b), show that the corrosion rates decreased by heat treatment (quenching regime). The quenching regime transformed the pearlitic-ferritic phase to martensite phase as described before, where small ferrite particles distributed in between cementite laminas. All ferritic area (in grain boundary and of ferrite laminas) are converted to small particles and distributed in between partitioned cementite laminas, so the anodic area (ferritic area) is increased by heat treatment
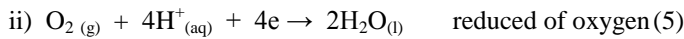
relative to cathodic area. Therefore, the decreasing of corrosion rate is attributed to cathodic area i.e. cathodic control (in absence of inhibitor).

Corrosion behavior in (H$_2$SO$_4$) solutions

The corrosion of carbon steel in aerated acid solution is a result of partial anodic reaction which involves the oxidation of metal atoms, and forms (Fe^{2+}) solution. The iron in anodic site is dissolved in H$_2$SO$_4$ solution as [20];
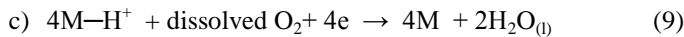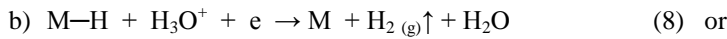
$$Fe + H_2SO_{4\ (aq)} \rightarrow FeSO_{4\ (aq)} + 2H^+ + 2e \qquad (2)$$

i.e. $Fe \rightarrow Fe^{2+} + 2e$ \qquad (3)
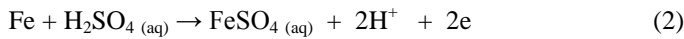
At cathodic sites in presence of aerated oxygen; two types of cathodic reaction may be occurred in acid solution [19].

i) $2H^+ + 2e \rightarrow H_2$ \qquad hydrogen evolution \qquad (4)

ii) $O_{2\ (g)} + 4H^+_{(aq)} + 4e \rightarrow 2H_2O_{(l)}$ \qquad reduced of oxygen (5)

The corrosion rate increases as the acid concentration increases due to increasing of adsorbed hydrogen ions on the metal surface where an electro chemical reaction takes place in presence of O$_2$ as;

$$M + H_3O^+ + e \rightarrow M{-}H + H_2O \qquad (6)$$

Where three steps can be done as;

a) $2M{-}H \rightarrow 2M + H_{2(g)}\uparrow$ \qquad (7)

b) $M{-}H + H_3O^+ + e \rightarrow M + H_{2\ (g)}\uparrow + H_2O$ \qquad (8) or

c) $4M{-}H^+ + dissolved\ O_2 + 4e \rightarrow 4M + 2H_2O_{(l)}$ \qquad (9)

The corrosion rates at 25°C in presence of 10% ethanol that mixed with 0.1, 0.5 and 1.0 N H$_2$SO$_4$ increase in the order 0.1< 0.5<1N for all samples; LCA, MCA, LCH and MCH (i.e. before and after heat treatment) see (Table 3) and (Fig 5 & 6).

These behaviors can be discussed in view of all processes that occur at anodic and cathodic sites which described before.

Effect of concentration of ethanol on corrosion behavior

In presence of constant concentration (0.1 N) H$_2$SO$_4$, it is obvious that the corrosion rates decrease as the concentrations of ethanol increased for all samples (i.e. before and after heat treatment) see (Figs 5 & 6), and (Tables 3). These behaviors in the same order of the dielectric constant of mixed solutions see (Table

5), that decreased in the order: 10% > 20 % > 30 %. This result clarifies the retarding effect of the dielectric constant in the corrosion rate.

In spite of the dielectric constant of mixed solution (constant concentrations of H_2SO_4, and ethanol) decreases as the temperature increase in the order; 15Cº > 25Cº > 35Cº > 45Cº > 55Cº the rate of corrosion increased. This result indicates that accelerated effect of temperature on acid behavior is more than the retarding effect of the dielectric constant or ethanol concentration.

From (Figs 5&6), it observed that the corrosion curve has concave shape in the case of low carbon while it has convex shape in medium one. It indicates that the corrosion rate of medium carbon steel in dilute acid solution is faster than in concentrated one, while this behavior has reversed action on the low carbon steel.

Effect of temperature on the corrosion behavior

The corrosion rates in presence and absence of (HEAA) increased with increasing the temperature in the order;

$$15ºC < 25ºC < 35ºC < 45ºC < 55ºC$$

Inhibition efficiency of HEAA

The HEAA compound has six active centers as; two π – bonds (C== O) and (C==C) and four lone pair electrons (–N= and 3 O) all act as donor center.

Because of the restricted un-plainer structure of HEEAA, not all active group acts in the same time. These centers oriented to anodic sites (iron carbide) and adsorbed on it. The HEAA molecule attached with anodic site and covered somewhat of cathodic area, so that the corrosion rate in presence of HEAA is anodic-cathodic control.

The inhibition efficiency (IE %) is calculated as following [13].

$$IE\% = ((w - w')/w) \times 100$$

Where; w and w' are the weight loss in absence and presence of inhibitor respectively. The inhibition efficiency data in (Table 4), obvious that this inhibition efficiency for all samples under study increases with increasing HEAA concentration in the following order:

$$10^{-4} > 8x10^{-5} > 6x10^{-5} > 4x10^{-5} > 2x10^{-5} \text{ M of HEAA}$$

In all cases the inhibition efficiency decreased as the temperature of the medium is increased.

Relation between C % and inhibitor efficiency

This relation has two behaviors in before and after heat treatment.

Before heat treatment

The inhibition efficiency decreased as C% increased (Fig 7A) except at 2×10^{-5} M HEAA (has no sufficient concentration). A schema models were suggested to illustrate the C % effect.
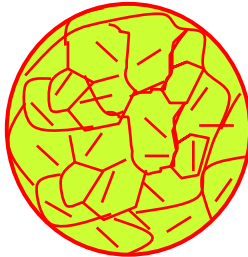
LCA   MCA

MCA has more ferrite phase (58%) than LCA, so it has more ferrite laminas in pearlite phase and thicker grain-boundary,
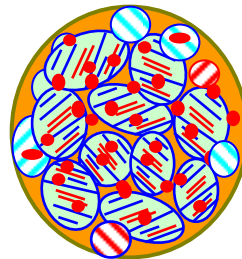
The corrosion rate in MCA is more dependent upon inter-granular corrosion type (IGC).

After heat treatment

The inhibition efficiency of LCH and MCH increased as C% increased (Fig 7B). A schema models were suggested to illustrate the heat treatment effect.

MCA   MCH

After heat treatment the ferrite is more distributed in martensite phase giving more anodic and cathodic sites. In this case the HEAA molecule can be covered

more cathodic sites than in the case before heat treatment, (i.e. IE% increased by heat treatment).

It observed that the corrosion rate of MCH is higher than in the case of LCH, and the IE % of MCH is higher than in the case of LCH too (Fig 7A). This behavior can be clarified in view of the effect of ferrite/cementite ratio is more than the inhibition effect in MCH where the corrosion rate in this case is more dependent upon AGC.

In general the IE is increased by heat treatment because of the ratio of (ferrite/cementite) area is changed and the type of corrosion is more dependent upon galvanic corrosion. It is sound that more cathodic area is covered by inhibitor where corrosion rate in presence of inhibitor is controlled by anodic-cathodic area.

The orientation of HEAA molecule to iron surface can be described by do a structure schema model as following. May be three or four donor centers only can be absorbed on anodic sites owing to restricted of the structure (see model).

Compare the (ferrite/cementite) in low and medium carbon steel and presented it as surface areas, the anodic – cathodic behavior of HEAA can be clarified.
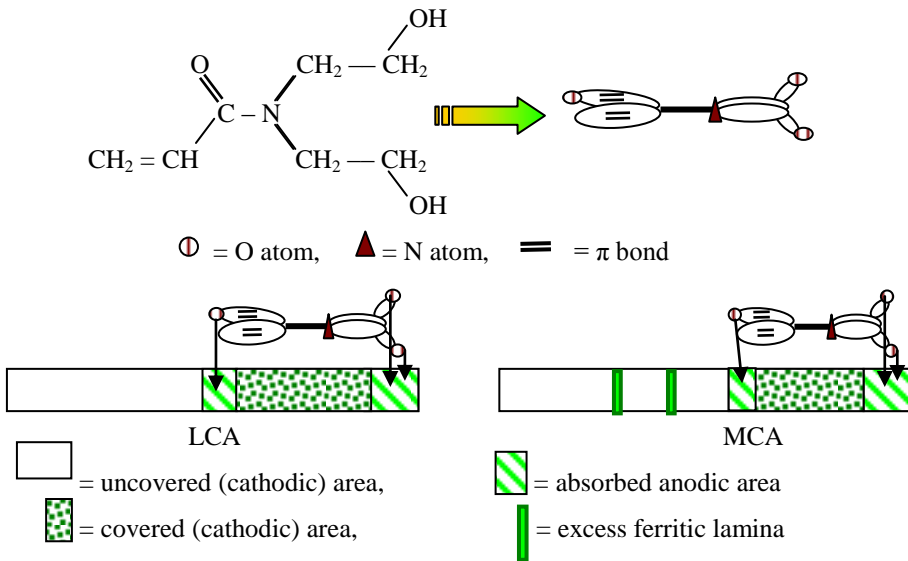
The uncovered cathodic area in MCA is more than the uncovered cathodic area in LCA and the excess ferritic laminas formed excess galvanic sites, i.e. the corrosion rate is increased by increasing the C% that increasing the AGC type.

Conclusion:

♦ The P% and Si% of LCA set the sample in moderate IGC sensitization region while P% of MCA sets the sample in no IGC sensitization region.

♦ Manganese and sulphur did not have any significant effect on the resistance to inter-granular attack.

♦ According to TTS curves the high fast cooling rate is very necessary to prevent IGC sensitization.

♦ The quenching heat treatment (in water) causes phase – transformation.

♦ Pearlite phase consists of two types of laminas (ferrite and cementite laminas) that transformed by heat treatment to martensite phase.

♦ The martensite phase has small ferrite particles and/or laminas that distributed in between partitioned cementite laminas.

♦ The corrosion rates for all samples in absence and presence of (HEAA) under studied conditions have same order; MCA> MCH> LCA> LCH.

♦ There are two wet corrosion processes that affected by carbon percent in the localized area. 1) IGC;   Fe, grain-boundary | wet medium | pearlitic grain, Fe

               2) AGC; Fe, Ferritic lamina | wet medium | cementite lamina,Fe

♦ The corrosion rates in absence of inhibitors classified as cathodic control.

♦ The decreasing of corrosion rate after heat treatment is attributed to decreasing of cathodic area.

♦ The corrosion rates in mixed solutions increased as acid concentration increased while it decreased as ethanol concentration increased which clarify the retarding effect of the dielectric constant.

♦ The accelerated effect of temperature on corrosion rate is more than the retarding effect of the dielectric constant.

♦ The corrosion rate of medium carbon steel in dilute acid solution is faster than in concentrated one, while this behavior has reversed action on the low carbon steel.

♦ Because of the restricted un-plainer structure of HEEAA, not all active group acts in the same time and the corrosion rate in presence of HEAA is anodic-cathodic control.

♦ Before heat treatment the corrosion rate in MCA is more dependent upon inter-granular corrosion type (IGC) owing to it has more ferrite phase (58%) than LCA, so it has more ferrite laminas in pearlite phase and thicker grain-boundary.

♦ IE% increased by heat treatment where the HEAA molecule can be covered more cathodic sites than in the case of before heat treatment.

Tables

Table (1)- Chemical composition of steel samples and its symbols.

Type	C%	Mn%	S%	P%	Fe%	Si%	as cast	heat treated
Low; C	0.24	0.85	0.057	0.05	98.6	0.24	LCA	LCH
Medium;C	0.38	1.23	0.018	0.019	98.1	0.24	MCA	MCH

Table (2) : Composition of corrosive medium.

Ethanol %	10 %			20 %			30 %		
H_2SO_4 (N)	0.1 N	0.5 N	1.0 N	0.1 N	0.5 N	1.0 N	0.1 N	0.5 N	1.0 N
symbol	A1	A2	A3	B1	B2	B3	C1	C2	C3

Table (3): Corrosion rate data in absence of inhibitor were recorded.

Corrosive media	Rate of Corrosion (mm/y)			
	As Cast		Heat Treated	
	LCA	MCA	LCH	MCH
A1	20.52	25.24	18.95	22.10
A2	28.42	50.52	26.84	37.87
A3	53.68	63.14	44.20	48.93
B1	18.95	20.54	17.37	18.92
B2	26.84	44.22	25.26	33.13
B3	44.20	56.81	41.04	44.19
C1	12.63	17.36	7.89	12.62
C2	25.26	39.45	23.68	26.83
C3	41.04	44.19	37.89	39.45

Table (4);Corrosion rate data in presence of (4 x10^{-5} M) inhibitor at 25°C.

Corrosive media	Rate of Corrosion (mm/y)			
	As Cast		Heat Treated	
	LCA	MCA	LCH	MCH
A2	15.80	31.57	13.00	17.36
IE %	44.41	51.57	37.51	54.16

Table (5);Dielectric constant of ethanol at deferent temperatures.

Concentration of ethanol	Dielectric constant				
	15C^o	25C^o	35C^o	45C^o	55C^o
10%	76.10	72.80	69.42	66.20	62.70
20%	70.10	67.00	63.97	60.80	57.50
30%	64.00	61.10	58.01	55.20	52.50

Figures

Phase diagram of Fe – Fe$_3$C
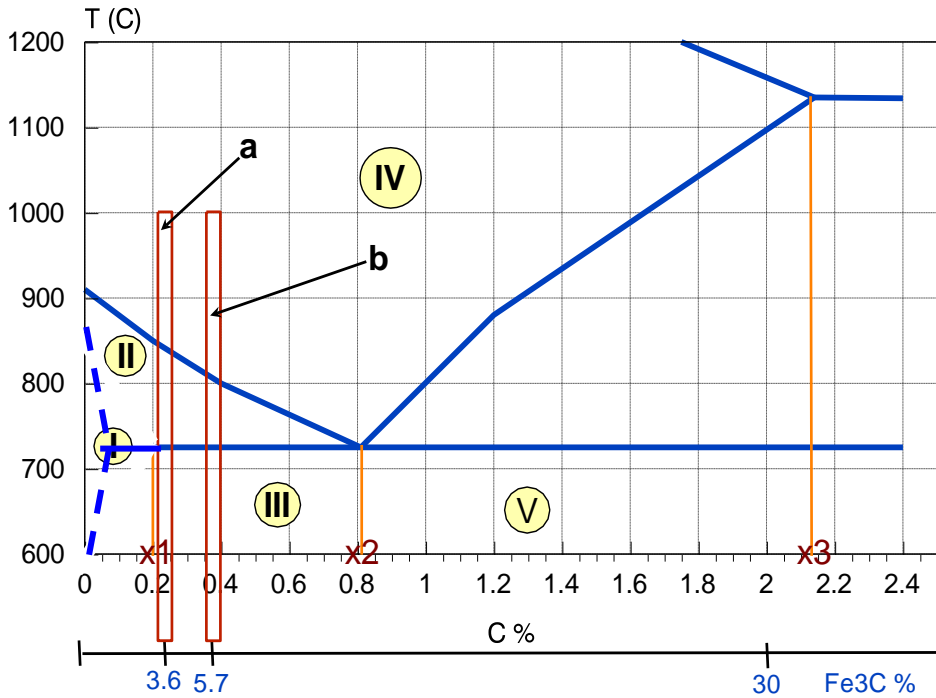
Fig; (1): The Fe – Fe$_3$C equilibrium diagram.

Where:
 (I) = Ferrite phase.
 (II) = Austenite + ferrite phase.
 (III) = Ferrite + Pearlite phase.
 (IV) = Austenite phase.
 (V) = Cementite + pearlite phase.
 (x1) = At 0.2 % Carbon (the first eutectic point) is allocated to ferrite + cementite (tertiary) phase.
 (x2) = At 0.81 % Carbon (the second eutectic point) is allocated to pure pearlite phase.
 (x3) = At 2.14 % Carbon (the third eutectic point) is allocated to pure ledeburite phase.
 (a) = The heat treatment area of low carbon steel under study.
 (b) = The heat treatment area of medium carbon steel under study.
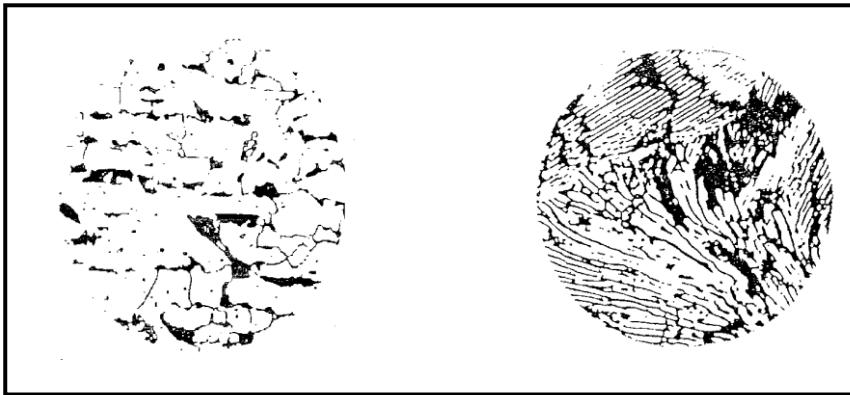
i (LCA)   ii (MCA)

Fig (2): Microscopic scan for LCA and MCA as cast.
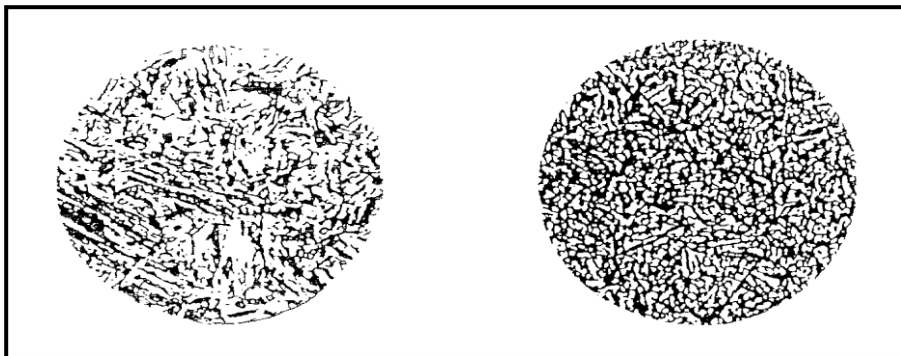
iii (LCH)   iv (MCH)

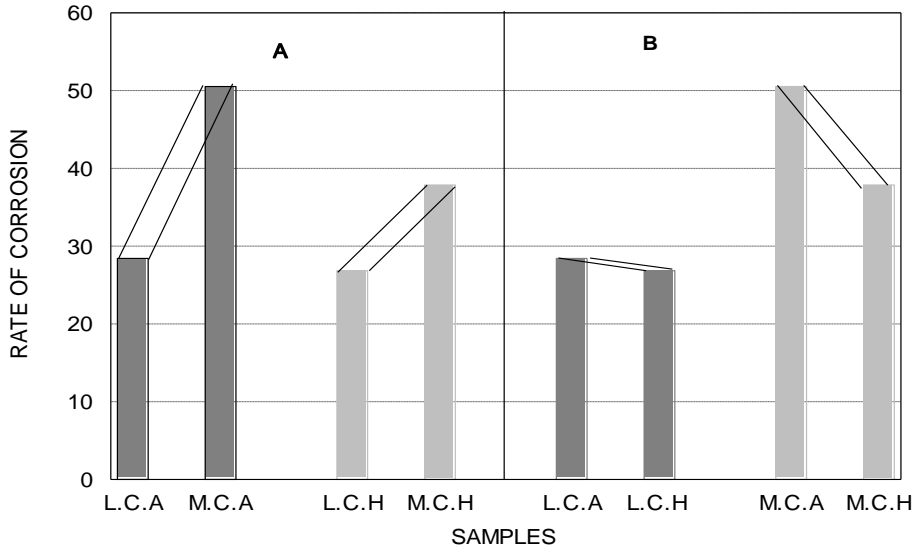**Fig (3): Microscopic scan for LCH and MCH (heat treated).**

Fig (4): Relation between corrosion rate and;
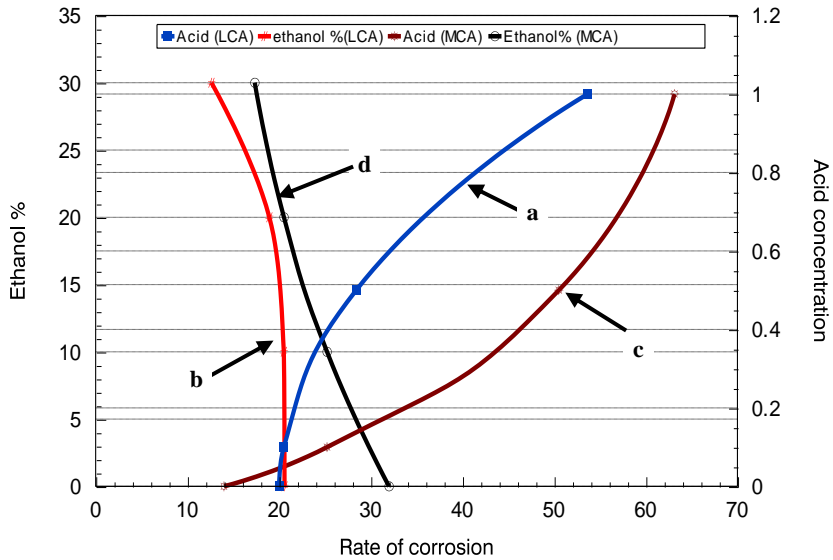
A)   Carbon percent.   B) Heat treatment.

**Figure (5): The effect of medium concentration on the corrosion
rates of LCA & MCA samples**
(a & c) in 0.5N H_2SO_4 with different concentration of ethanol.
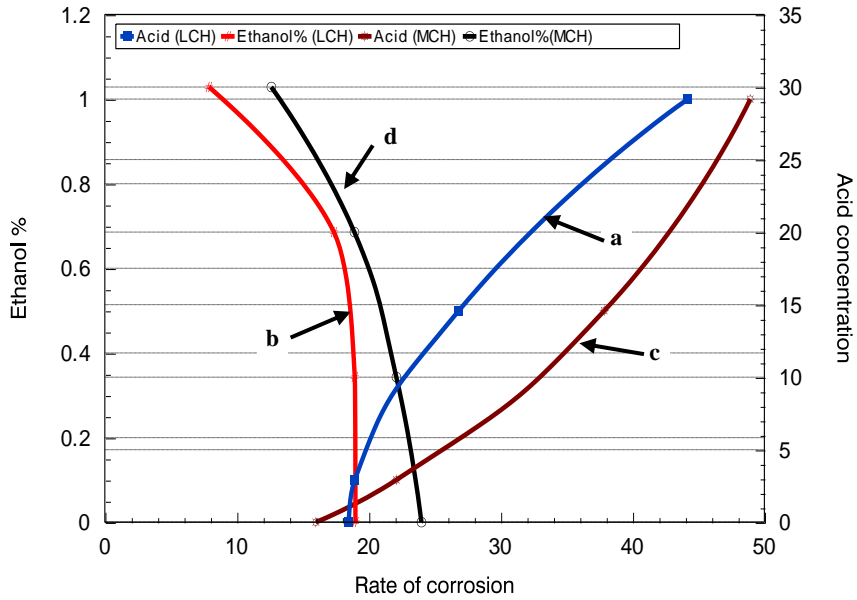(b & d) in 10 % ethanol with different concentrations of H_2SO_4.

Figure (6): The effect of medium concentration on the corrosion rates of LCH & MCH samples

(a & c) in 0.5N H_2SO_4 with different concentration of ethanol.

(b & d) in 10 % ethanol with different concentrations of H_2SO_4.
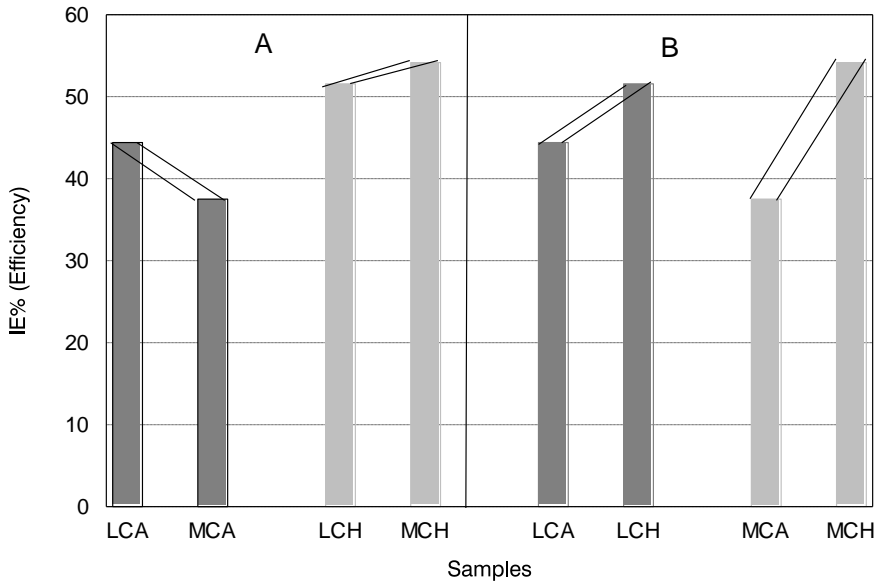

Figure (7): The relation between IE % and steel microstructure.

References:

1. Galal, N. F. Atta and M. H. S. Al-Hassan; Material chemistry physics; V89; P38-48 (2005).

2. S.R. Selim, Al-Azhar Bull. Sci,.12, 87 (2001).

3. M. salasi, T. shahrabi, E. Roayaei and M. Aliofkhazraei; Material chemistry and Physics, Accepted (2007).

4. W.leslie; Physical Metallurty of Steel; Mc Graw – Hill, New Yourk, 1981.

5. S.R. Selim, and S.H. El-Nekhaly, Modeling Measurement and Control, France, 60, 28 (1999).

6. Y. Abboud, A. Abourriche, T. Saffaj, M. Berrada, M. Charrouf, A. Bennamara, N. Al Himidi and Hannache, Material Chemistry physics; V105; P1-5(2007).

7. A. Popova, M. Christov and A.vasilev; Corrosion Science; V49,P3276-3289 (2007).

8. Y. Abboud, A. Abourriche, T. Saffaj, M. Berrada, M. Charrouf, A. Bennamara, A. Cherqaoui and D. Takky; Applied Surface Science; V252, P8178-8184 (2006).

9. A. M. Abdel-Gaber, B. A. Abd El-Nabey, I. M. Sidahmed, A.M. El-Zayady and M. Sadawy, Corrosion Science; V48, P2765-2779 (2006).

10. Mu. Guannan, Li. Xianghong, Qu. Qing and Jun. Zhou; Corrosion Science; V48; P445-459 (2006).

11. A. A. Mohamed and F. Abd El-Hai, European Coating, Journal, 38 (2004).

12. S.R. Selim, Al-Azhar Bull. Sci., 4, 21(1993).

13. M. lebrini, M. Lagrenee, M. Traisnel, L. Gengembre, H. Vezin and f. Bentiss; Applied Surface Science, V253,P9267-9276 (2007).

14. M. M. El-Naggar; corrosion Science; V49, P2226-2236 (2007).

15. P. B. Raja and M. G. Sethuraman; Materials Letters; V62, P1602-1604 (2008).

16. S.R. Selim, M.F. El-Hady, M.M.B. Awad and A.A. El-Zomrawy Al-Azhar Bulletien of science, proceeding of the 4th Int. Sci. Conference march, PP181-198 (2001).

17. A. A. Mohamed, S. H. El-Nekhaly and M. F. Bakr, Mans. Sci. bull. (A Chem.), 31(1), 67 (2004).

18. Raj Narayan An Introduction to Metallic Corrosion and its Prevention, Oxford, New Delhi, P73 (1983).

19. R. E. Reed – Hill ; Physical Metallurgy Principles; Brook And Cale Engineering Division, Monterey, California, (1973).

20. M. Pourbaix, "Atlas of Electrochemical Equilibria, in Aqueous Solutions", Pergamon Press, Oxford (1966).